Dynamics of Ion–Molecule Reactions

BRUCE H. MAHAN

Inorganic Materials Research Division of the Lawrence Radiation Laboratory and Department of Chemistry, University of California, Berkeley, California

Received April 17, 1968

In recent experiments the energy and angular distributions of the products of ion–molecule reactions have been determined. Analysis of these data show that, for $N_2^+ + D_2 \rightarrow N_2D^+ + D$ and other related hydrogen-abstraction reactions, most of the products are formed with very high internal excitation by grazing collisions. Very large isotope effects are found and can be understood in terms of product internal excitation and stability with respect to dissociation. In studies of nonreactive but inelastic ion–molecule collisions, clear evidence of electronic and vibrational excitation processes has been found. These data begin to give us a picture of the detailed dynamics of chemical reactions and inelastic collisions.

The goal of investigations of molecular dynamics is to obtain a detailed description and understanding of how molecular systems are transformed from one state to another. A large variety of processes are currently under study: the unimolecular processes of decomposition and rearrangement, bimolecular phenomena including collisional excitation of electronic, vibrational, and rotational levels as well as chemical transformations, and termolecular recombination reactions. The present state of the molecular dynamics field is similar to what must have prevailed in the areas of molecular spectra and structure in the early 1930's—the theoretical formalism necessary for interpretation is largely available, but often not in usable form, and initial work has suggested a wealth of refined, and we hope revealing, new experiments.

The very substantial recent progress in reaction kinetics really started when experimentalists began to isolate and study elementary reactions—simple processes in which three or fewer molecules participate. Investigation of these elementary processes gives us reaction rate constants whose values are known as a function of temperature. This information is very valuable, since it can be used to unravel or even to predict the reaction mechanisms of complicated systems, or at the very least to select the reactions which may or may not be of importance in an uninvestigated reaction mixture.

Unfortunately, the magnitude and temperature dependence of the rate constant reveal rather few details of the reaction dynamics. The value of the activation energy gives only a slight hint of what the potential energy surface for a bimolecular reaction is like. The comparison of the measured preexponential factor with values calculated by absolute rate theory can indeed be used to reject some models for the reaction transition state. However, the kinetic data are usually consistent with a substantial number of sets of reasonable bond distances, angles, and vibrational frequencies for the transition state. The danger of attempting to "invert" kinetic data to obtain values for these many parameters from essentially one experimental quantity should be obvious, but is all too often ignored.

It is clear that, to learn more about potential energy surfaces and reaction dynamics, we must measure more than the reaction rate constant. Kinetic spectroscopy allows examination of reaction products shortly after their formation by means of time-resolved ultraviolet or infrared spectra and potentially offers very significant information about reaction dynamics. The results and interpretation of these experiments are sometimes complicated, however, by nonreactive but inelastic collisions which change the population of product states from that produced by the reaction. It is clear that measurements made on the products of a bimolecular reaction before such thermalizing collisions occur will be most revealing. This fact is one of the motivations for the molecular beam approach to chemical kinetics. The method is restrained only by the concomitant low intensities which limit the details that energy and momentum analyzers, state selectors, and spectroscopic detectors can discern. In this article I shall describe our use of molecular beam techniques in investigations of ion–molecule reaction dynamics.

Gaseous ion–molecule reactions have been known since the very early days of mass spectrometry.[1] Only in the past 10 years have they come under intensive investigation, following the initial stimulation of Tal'rose, Lindholm, Stevenson and Schissler, and Field and Franklin. There have been several related experimental techniques employed. First studies were made simply by raising the pressure in the ion source of a mass spectrometer, and secondary ions formed by reaction were identified by chemical arguments, appearance potentials, and dependence of their intensities on source pressure and repeller voltage. This technique has led to the discovery of more reactions and the measurement of more reaction cross sections than any

(1) For reviews of this field, see (a) F. W. Lampe, J. L. Franklin, and F. H. Field, *Progr. Reaction Kinetics*, **1**, 69 (1961); (b) V. L. Tal'rose, *Pure Appl. Chem.*, **5**, 455 (1962); (c) C. E. Melton in "Mass Spectrometry of Organic Ions," F. W. McLafferty, Ed., Academic Press, Inc. New York, N. Y., 1963, Chapter 2; (d) D. P. Stevenson in "Mass Spectrometry," C. A. McDowell, Ed., McGraw-Hill Book Co., Inc., New York, N. Y., 1963, Chapter 13; (e) C. F. Giese, *Advan. Chem. Phys.*, **10**, 247 (1966); (f) "Ion-Molecule Reaction in the Gas Phase," Advances in Chemistry Series, No. 58, American Chemical Society, Washington, D. C., 1966.

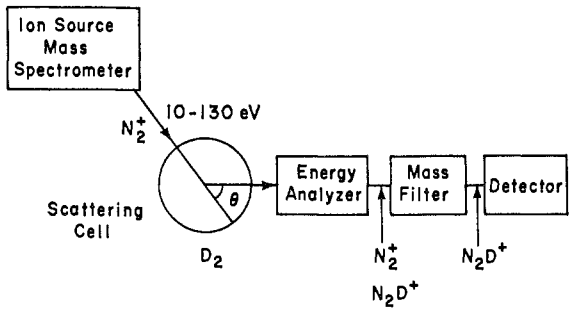

Figure 1. A block diagram of the apparatus used to study the dynamics of ion–molecule reactions. The composition of the ion current at various stages is indicated.

other. Its drawbacks are that it gives relatively little unequivocal information about reaction dynamics and can be ambiguous when one product ion can be formed by two or more reactions of the same order, as, for example, in

$$Ar^+ + D_2 \longrightarrow ArD^+ + D$$
$$Ar + D_2^+ \longrightarrow ArD^+ + D$$

Use of tandem mass spectrometers[2-4] largely avoids ambiguities of reaction mechanism. The first mass spectrometer is used to prepare ions of known mass which then impinge on the reactant gas in the source of a second analytical mass spectrometer used to detect the secondary ions. The tandem spectrometer technique allows one to determine the reaction cross section for primary ions at a series of known energies.

The foregoing methods do not involve an analysis of the energy distribution of product ions nor of their angular distribution with respect to the direction of the primary ion motion. Molecular beam studies[5] of reactions between neutral molecules have shown how the product energy and angular distribution can reveal the reaction dynamics. For this reason, we constructed an apparatus in which a collimated beam of ions of known mass and energy could be directed into a target gas, and the mass, energy, and angle of product and scattered reactant ions could be determined.[6] In at least two other laboratories[7,8] somewhat similar instruments have been completed and are in operation. A number of others are under construction.

Figure 1 shows a block diagram of our instrument. The primary mass spectrometer is a fairly conventional magnetic sector instrument with a high-intensity ion source, high-order focusing, and a lens system for rendering the ion beam parallel. Nearly all our experiments have been done with the target gas contained in a cylindrical scattering cell. This cell can be replaced by a molecular beam, and will be in our future experiments. For the type or experiments we are now doing, using a beam of neutral molecules offers few advantages and would be accompanied by a serious loss of product intensity.

Ions which pass through the exit aperture of the scattering cell enter an electrostatic energy analyzer, which transmits ions of a selected kinetic energy, regardless of their mass. These energy-analyzed ions move into a quadrupole mass filter where the desired ion is selected and then detected by an ion-to-electron converter followed by a low-energy β-ray counter. The exit aperture of the scattering cell and the whole detection train can be rotated through known angles with respect to the incident ion beam, and thus the intensity of any ion as a function of its speed and angle can be measured.

What do we expect the distributions of scattered particles to look like, and how can we interpret them? To find the answer, we first consider the scattering in a simple nonreactive system, N^+ projectiles on helium gas. In a typical experiment we would use N^+ ions of 60-eV energy which would have a velocity of 2.9×10^6 cm/sec, while the root-mean-square velocity of the target He atoms at room temperature is only 1.4×10^5 cm/sec. Thus as an acceptable first approximation we can consider the He atoms to be stationary and construct the velocity vector diagram of Figure 2. Here the velocity of He is represented as a point at the origin of a stationary or laboratory coordinate system, and the initial velocity of the projectile N^+ ions is taken to be v_{N^+}.

The two-particle-system N^+–He has a center of mass which lies closer to N^+ than to He because of the greater mass of N^+. The center of mass moves with a constant velocity regardless of the occurrence and nature of the collision, be it elastic, inelastic, or reactive. Therefore, the motion of the center of mass contains no information about the interaction between the two collision partners. However, the details of the molecular interaction do affect the motion of the particles *relative* to their center of mass. Consequently, it is advantageous to analyze a collision by using a coordinate system which has its origin at, and moves

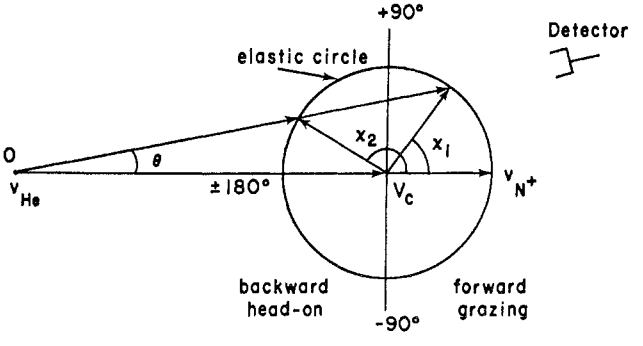

Figure 2. A velocity vector diagram for the N^+–He collision. The elastic circle is the locus of all possible velocities for elastically scattered N^+.

(2) C. F. Giese and W. B. Maier, *J. Chem. Phys.*, **35**, 1913 (1961).
(3) M. A. Berta and W. S. Koski, *J. Am. Chem. Soc.*, **86**, 5098 (1964).
(4) J. H. Futrell and F. P. Abramson in ref 1f, p 107.
(5) D. R. Herschbach, *Advan. Chem. Phys.*, **10**, 319 (1966).
(6) W. R. Gentry, E. A. Gislason, B. H. Mahan, and C. W. Tsao, *J. Chem. Phys.*, **47**, 1856 (1967).
(7) L. D. Doverspike, R. L. Champion, and T. L. Bailey, *ibid.*, **45**, 4385 (1966).
(8) Z. Herman, J. D. Kerstetter, T. L. Rose, and R. Wolfgang, *ibid.*, **46**, 2844 (1967).

with, the center of mass. The tip of the center-of-mass velocity vector V_c shown in Figure 2 thus forms the origin of the center-of-mass (CM) polar coordinate system, and the zero angle is conventionally taken to be the original direction of the ion beam.

An elastic collision is one in which the speed (but not the velocity vector) of each particle *relative to the center of mass* is the same before and after the collision. Therefore, the locus of possible final velocity vectors for elastically scattered N^+ is the circle shown in Figure 2, whose radius is just the initial speed of N^+ relative to the center of mass. Similarly, the final velocity vectors for elastically scattered He lie on a concentric circle of larger radius, since He, although stationary in the laboratory coordinate system before the collision, was moving more rapidly relative to the center of mass than was N^+.

By centering our attention on the elastic circle for N^+, we see why both energy and angular analysis of the products is desirable. With the detector set at the laboratory angle θ indicated in Figure 2, two kinds of N^+ ions would reach the detector: "fast" ions which had undergone a small deflection, χ_1, in the CM system, and "slow" ions which had been scattered through the larger angle χ_2. Ions are scattered through small CM angles ($|\chi| < 90°$) almost exclusively by grazing collisions in which the partners interact relatively weakly, whereas ions observed at CM angles greater than 90° come from more nearly head-on collisions. Kinetic energy analysis allows us to measure the intensities of these two groups of ions separately.

Kinetic energy analysis also permits us to detect the occurrence of inelastic and superelastic collisions. Ions whose velocity vectors are found to be inside the elastic circle must have undergone inelastic collisions, converting some of their initial kinetic energy into internal excitation energy. Similarly, primary ions which have excess internal energy may convert this to relative translational energy in a superelastic collision and will be found outside the elastic circle.

Figure 3 shows an experimentally determined intensity contour map of N^+ which has undergone collision with He. The most prominent feature is the elastically scattered N^+ which is distributed about the elastic circle (labeled $Q = 0$), just as expected. We were unable to detect elastic scattering at large angles in this experiment because this scattering is always intrinsically weak and in this case is further attenuated by competing inelastic processes. The peak just forward of the center of mass results from one of these inelastic processes. From its location relative to the center-of-mass velocity, we can tell that it is due to

$$N^+(^3P) + He \longrightarrow N^+(^3D) + He \qquad Q = -11.4 \text{ eV}$$

Here the quantity Q is the difference between the final and initial relative kinetic energy of the collision partners and in this case is just the negative of the internal excitation energy of the products. The maximum intensity of the peak in Figure 3 falls almost exactly

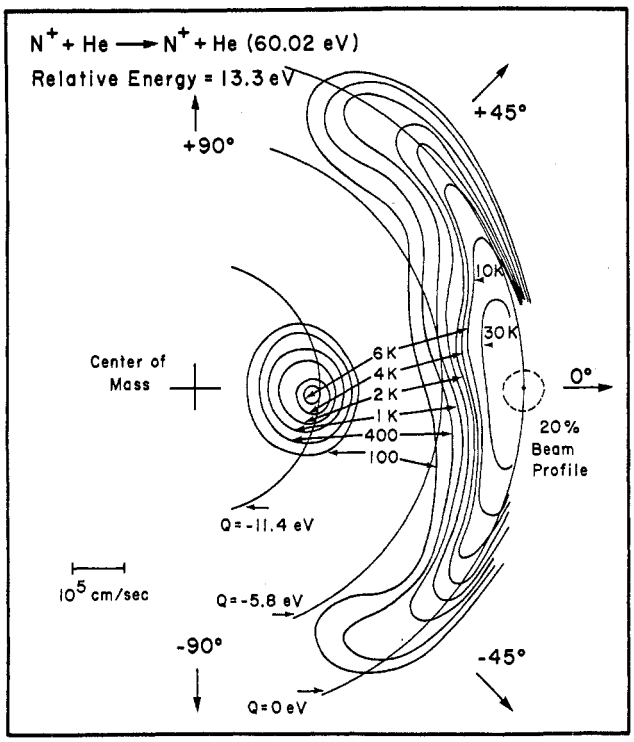

Figure 3. A contour map in the center-of-mass coordinate system of the relative intensity of N^+ scattered from He. The slight asymmetry about $\chi = 0$ arises from unavoidable stray fields and perhaps the intrinsic asymmetry of the magnetic momentum analyzer. The dashed line gives the profile of the ion beam at 20% of its maximum intensity. The quantity Q is the change in relative translational energy of the collision partners.

on the circle calculated for $Q = -11.4$ eV.

The distribution of elastically scattered N^+ shows a thickening near $\chi = 0°$, and noticeable intensity is present on the $Q = -5.8$ eV circle. This suggests that another inelastic process is going on, and, in fact, under other experimental conditions the excitation

$$N^+(^3P) + He \longrightarrow N^+(^5S) + He \qquad Q = -5.85 \text{ eV}$$

can be resolved clearly. We have less clear evidence that as many as five other electronic transitions occur in these collisions.

The mechanism by which electronic excitation of N^+ occurs is evidently the inverse of the collisional quenching of electronic fluorescence. That is, at some internuclear separations the potential energy curve for $N^+(^3P)$ + He crosses or comes very close to the ones that separate to $N^+(^5S)$ + He and $N^+(^3D)$ + He. Any potential energy curves constructed from theory should be consistent with this observation. Another description of the excitation process follows when it is realized that the ground state of N^+ has the electron configuration $2s^22p^2$, while the ^5S and ^3D states belong to $2s^12p^3$. We can say that the collision temporarily mixes the 2s and 2p orbitals of N^+ as the bonding, nonbonding, and antibonding σ orbitals of HeN^+ are formed. An electron initially in the 2s orbital of N^+ could therefore end up in the 2p orbital after the collision. The fact that electron spin is not conserved

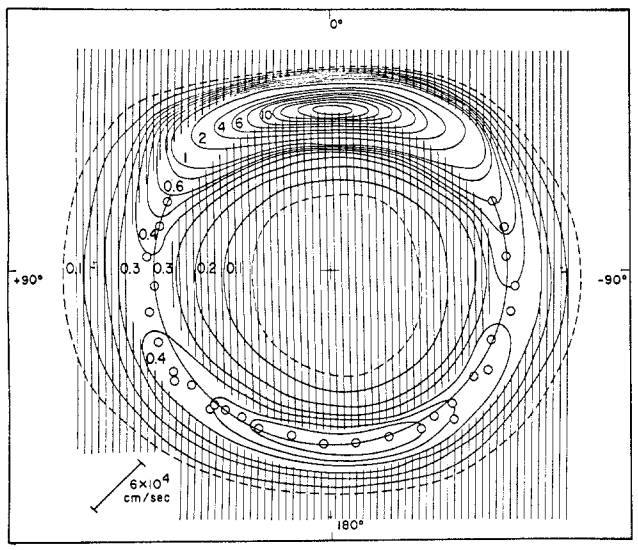

Figure 4. A contour map in the center-of-mass coordinate system of the relative intensity of N_2D^+ product from the N_2^+–D_2 reaction. The initial relative kinetic energy was 8.1 eV. The shaded areas are regions of velocity space forbidden by energy conservation and product stability. The small circles represent the actual intensity maxima that were located in experimental scans of angle at fixed energy and energy at fixed angle.

in the $^3P \rightarrow {}^5S$ transition is an interesting point and shows us that, even in a system as light as HeN^+, spin–orbit coupling is great enough to mix states of different spin if they become degenerate or nearly so.

This brief experience with atomic ion–atom scattering has convinced us that continuation, extension, and refinements of these experiments can teach us a great deal about the potential energy curves of diatomic molecules. In particular, molecules which do not have stable ground states can be studied, and energy levels reached only with great difficulty by spectroscopy are easily accessible.

We can now turn to the problem of collisions in which atom transfer occurs. The reaction which we and others[7-10] have studied most intensively is

$$N_2^+ + D_2 \longrightarrow N_2D^+ + D \qquad (1)$$

and its isotopic variations. The problem of predicting the allowed final velocities of N_2D^+ is a bit more complicated than was true for the N^+–He problem. There is now associated with eq 1 an exothermicity of reaction, $W = -\Delta E_0°$, so for this reason alone we might expect that the relative kinetic energies of the products and reactants would differ. In addition, N_2D^+ has closely spaced vibrational and rotational levels and may be formed with a great deal of internal excitation energy, U. By energy conservation, the quantity Q, which is the change of relative translational energy, must equal the difference between the reaction exothermicity W and the internal excitation energy of the products U: $Q = W - U$. The maximum value of Q occurs when the internal excitation U is zero. The minimum value occurs when the product internal excitation is so great that the product molecules dissociate. When one product is atomic and the other molecular, as in reaction 1, the maximum value of U is D, the dissociation energy of the weakest bond in the molecule. Thus we have $W - D \leq Q \leq W$ or $-2.5 \leq Q \leq 1$ eV for reaction 1. Corresponding to this range of allowed Q values, there will be an allowed range of velocities of N_2D^+.

With these ideas in mind, we can turn to Figure 4, a map of the intensity of N_2D^+ from the N_2^+–D_2 reaction. The regions of velocity space forbidden by the energy considerations of the previous paragraph have been shaded.

The crater-like shape of the product intensity distribution is easily seen to be a consequence of the restricted values for Q. Products should not be found in the outermost shaded region because the exothermicity of the reaction is not great enough to put them there even if their energy were all present as relative translational motion. Products should not be found in the inner shaded region because N_2D^+ molecules moving that slowly must contain so much internal excitation energy they are unstable with respect to dissociation to N_2 and D^+. The fact that some product intensity is found in these regions is a consequence of the finite energy and angular resolution of our apparatus and our neglect of the motion of the target molecules in the analysis.

From the fact that the product distribution is asymmetric about 90° in the center-of-mass system we can conclude that the reaction proceeds by a so-called direct interaction, that is, an impulsive type of collision in which the collision complex lives no longer than about 10^{-14} sec, a vibrational period. A complex that lived several rotational periods (only 10^{-13} sec at these energies) would decay in random directions and give a product distribution symmetric about $\chi = \pm 90°$.

We see that the scattered N_2D^+ is most intense in the small-angle or so-called "forward" scattering regions. These regions are associated with *grazing* collisions, as illustrated in Figure 5a. Evidently it is quite easy for N_2^+ to pass by D_2, pick up a D atom, and proceed as N_2D^+ along a trajectory which deviates very little from that of the original N_2^+. Since N_2D^+ is deflected very little, from Newton's third law we know that the free D atom receives very little impulse as it loses its partner. This process, in which the freed atom seems merely to observe while its partner is torn away, is called *spectator stripping*. Results obtained in our laboratory as well as others indicate that something close to the stripping process is responsible for much of the reactive scattering in systems 1–4.

$$N_2^+ + D_2 \longrightarrow N_2D^+ + D \qquad (1)$$

$$N_2^+ + CH_4 \longrightarrow N_2H^+ + CH_3 \qquad (2)$$

$$N_2^+ + C_2D_2 \longrightarrow N_2D^+ + C_2D \qquad (3)$$

$$Ar^+ + D_2 \longrightarrow ArD^+ + D \qquad (4)$$

(9) B. R. Turner, M. A. Fineman, and R. F. Stebbings, *J. Chem. Phys.*, **42**, 4088 (1965).
(10) W. R. Gentry, E. A. Gislason, B. H. Mahan, and C. W. Tsao, *Discussions Faraday Soc.*, **44**, 137 (1967).

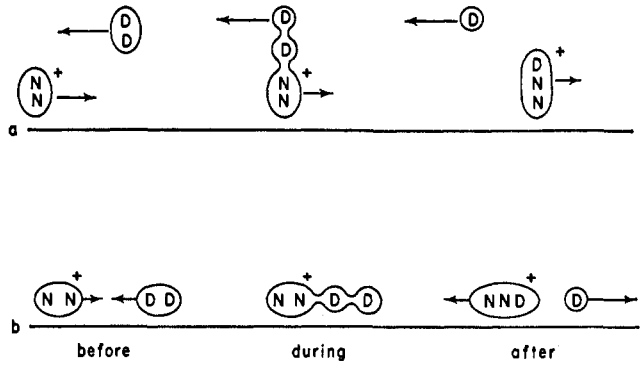

Figure 5. Schematic representation of reactive collisions: (a) a stripping process in which there is a grazing collision, and the trajectories of the N_2^+ moiety and the freed deuterium are little affected by reaction; (b) a rebound process in which the collision is nearly head-on, and freed D atom receives a large impulse.

The occurrence of the stripping process in this series of hydrogen-abstraction reactions is an interesting unifying feature. However, the prevalence of this mechanism at this time must not be overinterpreted. The grazing or large-impact parameter collisions associated with small angle scattering and stripping produce a large total reaction cross section. In selecting systems for our first experiments, we naturally pick reactions which have large cross sections, so that products will be easily observed. This process almost automatically selects reactions that display something close to the stripping phenomenon. In our most recent work we are studying eq 5, which has a noticeably smaller

$$N^+ + H_2 \longrightarrow NH^+ + H \qquad (5)$$

total cross section than reactions 1–4 and which shows a slightly less prominent stripping peak.

Returning to Figure 4, we see that, in addition to the small angle scattering, products are observed at large angles in the center-of-mass system. This backward or rebound scattering is associated with nearly head-on collisions between N_2^+ and D_2 in which the freed D atom receives a very large impulse. This process is illustrated in Figure 5b. Experiments in which we used a wide range of primary ion energies showed that the cross section for formation of N_2D^+ at all angles decreases as the collision energy increases, but that the rebound process increases in importance relative to the stripping process. The complete explanation for this is not obvious, but it may involve the fact that the rebound process provides a mechanism by which the internal energy of the product is kept below its dissociation energy.

Figure 4 shows that N_2D^+ formed by the stripping process has its greatest intensity right on the edge of the inner forbidden region of velocity space. This means that such molecules are internally excited almost to their dissociation limit. Any potential energy surface proposed for this reaction must be consistent with this observation. The detection of this high product excitation is important not only in analyzing the reaction dynamics but in predicting what the properties and eventual fate of the newly formed N_2D^+ will be in any complex reaction mixture.

Examination of the backward scattered products in Figure 4 shows that their intensity peaks somewhat away from the inner forbidden region of velocity space. This shows that back-scattered N_2D^+ is excited internally but has about 0.8 eV less internal energy than the forward-scattered N_2D^+. The recoil of the free D atom which accompanies back-scattering provides the mechanism for lowering the excitation energy of N_2D^+. The quantitative difference in the excitation level of forward- and backward-scattered products together with the angular variation of the intensities provide unique tests for any proposed potential energy surface.

Besides formation of N_2D^+, there are several other possible results of a collision between N_2^+ and D_2. Some of these are given by eq 6–9. The first two of

$$N_2^+ + D_2 \longrightarrow N_2 + D_2^+ \qquad (6)$$

$$N_2^+ + D_2 \longrightarrow N_2 + D^+ + D \qquad (7)$$

$$N_2^+ + D_2 \longrightarrow N_2^+ + D + D \qquad (8)$$

$$N_2^+ + D_2 \longrightarrow N_2^+ + D_2^* \qquad (9)$$

these (eq 6 and 7) have been observed by Bailey and Vance,[11] and at relative energies above about 3 eV they compete with reaction 1 to an important degree. Little is known of their detailed dynamics since it has not yet proved possible to measure simultaneously the energy and angular distribution of the products.

We believe that we have observed processes 8 and 9 by studying the energy distribution of N_2^+ scattered through small angles. Figure 6 shows the "translational energy spectrum" of 130-eV N_2^+ scattered through small angles by D_2. The value of Q for this nonreactive scattering gives the relative kinetic energy lost to internal excitation. We feel that the peak at -9 eV results from an excitation of D_2 to the $^3\Sigma_u$ state, which then dissociates to atoms.

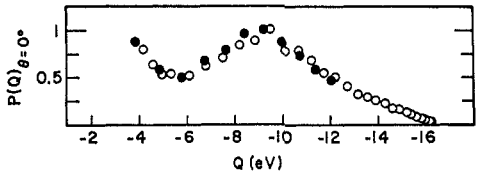

Figure 6. The probability $P(Q)$ of finding an N_2^+ ion which has been scattered with relative energy loss Q by D_2 as a function of Q. The initial relative energy was 16.3 eV. The results of two different experiments are shown by the open and closed circles.

The evidence for this interpretation is admittedly somewhat equivocal. The peak in question does not appear until the energy of N_2^+ is high enough to dissociate D_2, and as the energy of N_2^+ is increased, the Q value changes from -4.5 to -9 eV. This suggests

(11) D. W. Vance and T. L. Bailey, *J. Chem. Phys.*, **44**, 486 (1966).

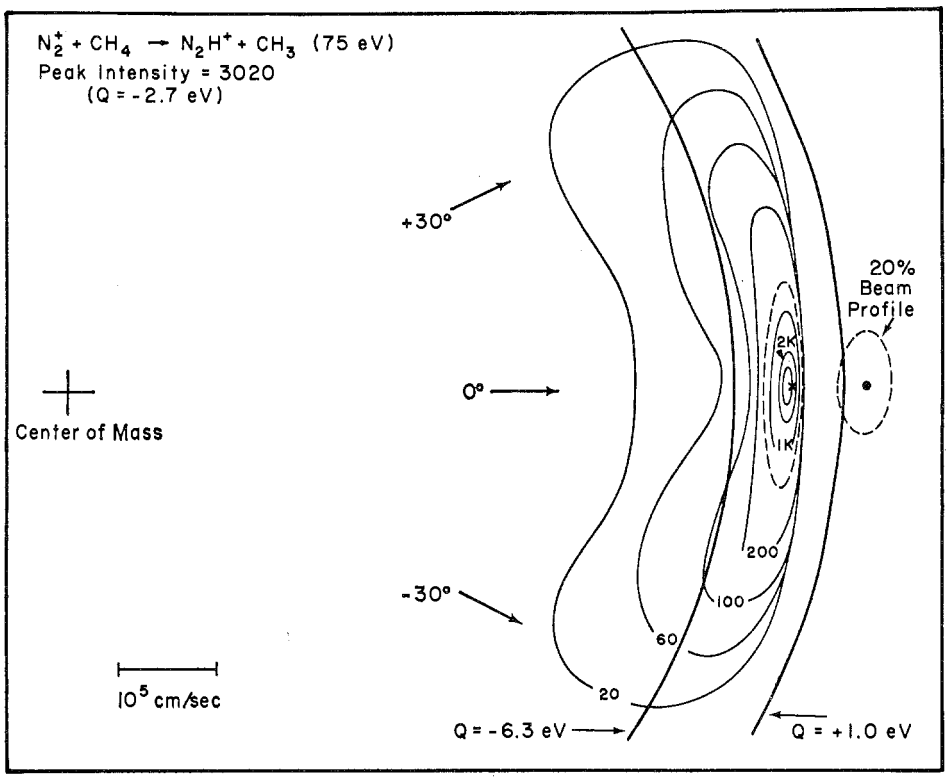

Figure 7. A contour map in the center-of-mass coordinate system of the intensity of N_2H^+ from the N_2^+–CH_4 reaction. The initial relative energy was 27.3 eV, the laboratory projectile energy 75 eV. The small cross at the intensity peak locates the velocity predicted from the ideal stripping mechanism.

to us that, upon approach of N_2^+, D_2 is distorted to larger internuclear separations and that, through an electron-exchange process, the lowest triplet of D_2 is formed. The threshold for this excitation is 4.5 eV if the D_2 is stretched to large internuclear separation. As the projectile velocities are increased, the distortion has less time to occur, the singlet to triplet excitation becomes more vertical, and the energy-loss spectrum peaks closer and closer to the vertical Q of -9 eV, as observed in Figure 6.

Another possible mechanism for dissociation is that N_2D^+ is formed by a stripping process but finds itself with so much internal energy it dissociates to $N_2^+ + D$. The N_2^+ from such events would appear near the peak found in Figure 6. However, this process is only possible at relative kinetic energies above 8.4 eV, and the inelastic peak referred to is observed at relative energies as low as 4.5 eV. Thus while it is possible for reaction followed by dissociation to contribute to reaction 8 at high energies, it definitely does not do so at low energies.

There is a third possible cause for the inelastic peak in Figure 6. It is possible that N_2^+ is being excited to one of its upper electronic states by collision with D_2. The N_2^+ does have a series of electronically excitated states whose excitation energies range from 1.1 to 8.0 eV, and these might be responsible for the continuous change in Q with increasing energy that we observe experimentally. However, we have not observed such energy losses in the scattering of N_2^+ by He, which suggests that the phenomenon we observe in the N_2^+–D_2 system is a consequence of the energy level pattern of D_2, not N_2^+. This argument is not particularly convincing, and by no means conclusive, so the matter remains uncertain for the present.

In Figure 6 we also see that appreciable N_2^+ is present between Q values of -2 and -4 eV. Some of the intensity is merely from the low-energy tail of our projectile beam, but the greater part of it is inelastically scattered N_2^+. We have observed similar inelastic scattering of N^+ from H_2 and believe it is due to vibrational excitation of the target H_2 or D_2 molecules.

From the N_2^+–D_2 reaction we turn to the related process

$$N_2^+ + CH_4 \longrightarrow N_2H^+ + CH_3 \qquad -\Delta E_0^\circ = W \cong 1 \text{ eV}$$

One of the maps which display the distribution of N_2H^+ is shown in Figure 7. The detectable scattering is confined to small (<30°) angles in the center-of-mass system, which indicates that the stripping model may be a good first approximation for this system as well. In fact, the most probable velocity of N_2H^+ is just about exactly the value calculated from the ideal stripping model. The calculated velocity for stripped products is indicated by the cross in Figure 7. This coincidence suggests that the methyl radical is completely oblivious to the hydrogen-atom abstraction.

The superficiality of this conclusion is revealed by

further inspection of the map of the N_2H^+ distribution. While the peak intensity does appear very near the ideal stripping velocity, which has a Q of -2.7 eV, a great deal of product intensity appears at even more negative values of Q. A Q value of -2.5 eV corresponds to enough internal energy to dissociate N_2H^+ if this energy were all concentrated in the ion. The fact that we see substantial product N_2H^+ in regions where Q is more negative than -2.5 eV means that much of the internal excitation energy of the products must reside in the methyl group, for if all this energy were concentrated in N_2H^+, it would surely dissociate and would not be detected. If Q is equal to or more negative than -6.3 eV, there must be 3.8 eV or more excitation energy in the methyl radical, which corresponds to the dissociation energy of the carbon–hydrogen bond. Thus we expect that, in the regions where Q is less than -6.3 eV, the methyl radial dissociates, and the actual reaction is

$$N_2^+ + CH_4 \longrightarrow N_2H^+ + CH_2 + H$$

At even higher relative energies we have found evidence that the methyl group fragments to CH and two hydrogen atoms.

We can now understand why we have been unable to detect product at large center-of-mass angles and speeds greatly different from the stripping velocity. The events which lead to large angle scattering are the nearly head-on collisions which occur with much smaller frequency than the grazing collisions which produce forward scattering or stripping. In these head-on collisions, the interaction is so violent that the methyl group will be fragmented, and up to four particles besides N_2H^+ may be formed in the collisions. With this many particles leaving in any direction, the momentum and energy conservation laws no longer confine the N_2H^+ to restricted regions of velocity space. Thus N_2H^+ formed from head-on collisions will be spread thinly throughout a very large region of velocity space and will not be detected by our device which samples only very small regions at a time.

The reaction of N_2^+ with CD_4 is similar to its reaction with CH_4 except that a very large isotope effect occurs. At a given projectile energy, N_2D^+ from CD_4 is much less intense and confined to much smaller scattering angles than is N_2H^+ from CH_4. At 50-eV projectile energy N_2H^+ may be 20 times more intense than N_2D^+, and at higher projectile energies the ratio becomes even larger. We have found equally large isotope effects for the forward-scattered or stripped products of the reaction of N_2^+ with H_2, D_2, and HD. Product ratios of this magnitude cannot be explained by the usual semiclassical treatment of isotope effects. There does seem to be a simple rationale, however, which involves the kinetic energy of the projectile relative to the abstracted atom. If the energy of the projectile of mass M and laboratory velocity v_0 is $^1/_2Mv_0^2$, its energy relative to a stationary atom of mass m is $^1/_2mMv_0^2/(M + m)$, or $m/(M + m)$ times smaller. Thus, at a given laboratory kinetic energy, a projectile has greater energy relative to a deuterium atom than to a hydrogen atom. If we compare the N_2H^+ and N_2D^+ intensities formed in experiments performed at the same energy relative to the atom abstracted, we find that the intensities are nearly the same. This holds for the reactions of N_2^+ with the isotopic hydrogen molecules as well as with CH_4 and CD_4. The isotope effect for forward scattering can be summarized by saying that the cross section for pick-up of H or D is the same at a given energy relative to the atom abstracted, and the cross section decreases as this energy increases.

According to the stripping model, the internal excitation (U) of the product ion is the sum of the exothermicity of reaction (W) and the energy of the projectile relative to the atom abstracted ($E_a°$): $U = W + E_a°$. Thus, at a given value of the projectile energy relative to the abstracted atom, N_2H^+ and N_2D^+ formed by the stripping process would have the same internal excitation. At a given laboratory projectile energy, however, $E_a°$ and U would be greater for N_2D^+ than for N_2H^+ according to this stripping model. At some critical projectile energy U will exceed the dissociation energy for N_2D^+ but not for N_2H^+. At this point the stripping model predicts an infinite isotope effect, since N_2D^+ should dissociate before detection. No such infinite effect is found, since the reactions do not conform exactly to the ideal stripping model. The measured velocities tell us that the products stabilize themselves by recoiling weakly off the freed atom. It appears that product intensity may be largely controlled by the requirement that, through recoils, the incipient N_2D^+ or N_2H^+ must lower its internal energy enough to be stable. At a given projectile energy this is always easier for N_2H^+, since it has started to form with less internal energy due to the smaller $E_a°$. Hence it is formed preferentially. At the same value of $E_a°$ for both isotopes the stabilization problem is the same, and there is no isotope effect.

Further support for the idea that the isotope effects are related to product internal excitation comes from our observation that, in the N_2^+–HD system, the isotope effect diminishes greatly in magnitude and then inverts in sense as the product scattering angle increases. Products scattered through large angles are less excited internally, and thus the differences in excitation between N_2H^+ and N_2D^+ do not influence the identity of the products strongly.

The experiments which I have described were among those performed during the first year that our apparatus was in operation. In the course of these preliminary experiments we have learned that several simple hydrogen-abstraction reactions proceed by a direct interaction rather than through a long-lived collision complex. Most of the products are scattered forward with very high internal excitation. Huge isotope effects are possible, and the magnitude and sense of the isotope effect are a function of the scattering angle. We have also observed a number of phenomena that

we feel deserve more detailed study. These include inelastic nonreactive processes, like the collisional electronic excitation of atomic projectile ions, and the vibrational excitation of small molecules and molecule ions. In the area of chemical reactions we intend to concentrate on studying the dynamics of reactions of atomic ions like Ar^+, O^+, N^+, C^+, F^+, and H^+ with diatomic molecules. We expect that for the simpler systems realistic potential energy surfaces will soon be calculated semiempirically or, as in the case of H^+–H_2, *ab initio*. At that point, it will become possible to make truly meaningful comparisons between theoretical and experimental reaction dynamics.

It is a pleasure to acknowledge the participation of Drs. Yuan-tseh Lee, W. R. Gentry, and E. A. Gislason and Messrs Chi-wing Tsao and Arthur Werner, who performed the experiments I have discussed. The work was supported by the U. S. Atomic Energy Commission, the Sloan Foundation, and the Chevron Research Company.